Are there reliable multiparametric MRI criteria for differential diagnosis between intracranial meningiomas and solitary intracranial dural metastases?

HONGJIE WU[1*], OZAL BEYLERLI[2,3*], ILGIZ GAREEV[2,3*], AFERIN BEILERLI[4], TATIANA ILYASOVA[5], RUSTAM TALYBOV[6], ALBERT SUFIANOV[7,8] and XIAOLONG GUO[1]

[1]Department of Neurosurgery, The First Affiliated Hospital, and College of Clinical Medicine of Henan University of Science and Technology, Luoyang, Henan 471003; [2]Department of Pharmacology (The State-Province Key Laboratories of Biomedicine Pharmaceutics of China, Key Laboratory of Cardiovascular Research, Ministry of Education), College of Pharmacy, Harbin Medical University, Harbin, Heilongjiang 150067; [3]Translational Medicine Research and Cooperation Center of Northern China, Heilongjiang Academy of Medical Sciences, Harbin, Heilongjiang 150081, P.R. China; [4]Department of Obstetrics and Gynecology, Tyumen State Medical University, Tyumen 625023; [5]Department of Internal Diseases, Bashkir State Medical University, Ufa, Republic of Bashkortostan 450008; [6]Department of Radiology, Federal Center of Neurosurgery, Tyumen 625062; [7]Department of Neurosurgery, Sechenov First Moscow State Medical University (Sechenov University), Moscow 119992; [8]Educational and Scientific Institute of Neurosurgery, Peoples' Friendship University of Russia (RUDN University), Moscow 117198, Russian Federation

Received February 2, 2023; Accepted May 30, 2023

DOI: 10.3892/ol.2023.13936

Abstract. Intracranial meningiomas are the most common tumors of the central nervous system (CNS). Meningiomas account for up to 36% of all brain tumors. The incidence of metastatic brain lesions has not been determined. Up to 30% of adult patients with cancer of one localization or another suffer from a secondary tumor lesion of the brain. The vast majority of meningiomas have meningeal localization; >90% are solitary. The incidence of intracranial dural metastases (IDM) is 8-9% of cases, while in 10% of cases, the brain is the only localization, and in 50% of cases the metastases are solitary. Typically, the task of distinguishing between meningioma and dural metastasis does not involve difficulties. Periodically, there is a situation when the differential diagnosis between these tumors is ambiguous, since meningiomas and solitary IDM may have similar characteristics, in particular, a cavity-less solid structure, limited diffusion of water molecules, the presence of extensive peritumoral edema, and an identical contrast pattern. The present study included 100 patients with newly diagnosed tumors of the CNS, who subsequently underwent examination and neurosurgical treatment at the Federal Center for Neurosurgery with histological verification between May 2019 and October 2022. Depending on the histological conclusion, two study groups of patients were distinguished: The first group consisted of patients diagnosed with intracranial meningiomas (n=50) and the second group of patients were diagnosed with IDM (n=50). The study was performed using a magnetic resonance imaging (MRI) General Electric Discovery W750 3T before and after contrast enhancement. The diagnostic value of this study was estimated using Receiver Operating Characteristic curve and area under the curve analysis. Based on the results of the study, it was found that the use of multiparametric MRI (mpMRI) in the differential diagnosis of intracranial meningiomas and IDM was limited by the similarity of the values of the measured diffusion coefficient. The assumption, previously put forward in the literature, regarding the presence of a statistically

Correspondence to: Dr Xiaolong Guo or Dr Hongjie Wu, Department of Neurosurgery, The First Affiliated Hospital, and College of Clinical Medicine of Henan University of Science and Technology, 24 Jinghua Road, Luoyang, Henan 471003, P.R. China
E-mail: guoxiaolong9999@126.com
E-mail: 39424561@qq.com

*Contributed equally

Abbreviations: IDM, intracranial dural metastases; CNS, central nervous system; MRI, magnetic resonance imaging; ROC, receiver operating characteristic curve; AUC, area under the curve analysis; mpMRI , multiparametric MRI; ADC, apparent diffusion coefficient values; CBF, cerebral blood flow; WHO, World Health Organization; MTT, mean transit time; ROI, the region of interest; PWI, perfusion-weighted imaging; DWI, diffusion-weighted imaging; ADC, apparent diffusion coefficient; SWAN, susceptibility-weighted angiography; IHC, immunohistochemical; SSTR2a, somatostatin receptor 2a; EH, epithelioid hemangioendothelioma; pPNET-ES, peripheral primitive neuroectodermal tumor-Ewing sarcoma

Key words: neuroimaging, mpMRI, MR perfusion, diffusion coefficient measurement, intracranial meningioma, biomarkers, intracranial dural metastasis

significant difference in the apparent diffusion coefficient values, which make it possible to differentiate tumors, was not confirmed. When analyzing perfusion data, IDM showed higher cerebral blood flow (CBF) values compared with intracranial meningiomas (P≤0.001). A threshold value of the CBF index was revealed, which was 217.9 ml/100 g/min, above which it is possible to predict IDM with a sensitivity and specificity of 80.0 and 86.0%, respectively. Diffusion-weighted images are not reliable criteria for differentiating intracranial meningiomas from IDM and should not influence the diagnosis suggested by imaging. The technique for assessing the perfusion of a meningeal lesion makes it possible to predict metastases with a sensitivity and specificity close to 80-90% and deserves attention when making a diagnosis. In the future, in order to reduce the number of false negative and false positive results, mpMRI would require additional criteria to be included in the protocol. Since IDM differs from intracranial meningiomas in the severity of neoangiogenesis and, accordingly, in greater vascular permeability, the technique for assessing vascular permeability (wash-in parameter with dynamic contrast enhancement) may serve as a refining criterion for distinguishing between dural lesions.

Introduction

Meningiomas are a group of tumors of the central nervous system (CNS) of meningothelial origin, and are the most frequently histologically diagnosed of all CNS tumors, accounting for ~36% of all CNS tumors (1). The 5th edition of the World Health Organization (WHO) classification of CNS tumors describes 15 histological subtypes of meningiomas and 3 prognosis grades (2). The majority of meningiomas are histologically benign (WHO Grade 1 2021) (1); 20-25% show atypical features (WHO Grade 2 2021); and the morphological parameters of 1-6% of meningiomas are associated with a less favorable clinical outcome and correspond to anaplastic tumor (WHO Grade 3 2021) (3-5). The morphological grade system describes the likelihood of recurrence. The frequency of recurrence of benign meningiomas reaches a quarter (7-25%), atypical, just over half (29-52%), and anaplastic (or malignant) meningiomas recur with a frequency ranging from 50-94% of cases (6).

CNS metastases are a group of tumors with a source of origin outside the CNS and a hematogenous route of spread; the true occurrence rate of which has not been determined and is probably underestimated (7). It is hypothesized that ~30% of adult and 6-10% of pediatric cancer patients suffer from a secondary brain tumor (8). Tumors and their molecular subtypes differ in their propensity to metastasize to the CNS; the most common source of brain metastases is lung cancer (most often adenocarcinoma), followed by breast cancer, melanoma, renal cell carcinoma, and colorectal cancer (9). Significant prognostic factors for patients with intracranial metastases are age, Karnofsky index, number of metastatic lesions, and severity of extracranial involvement (10).

The vast majority of meningiomas have a meningeal localization. Rarely, meningiomas may be intraventricular, epidural, or even occur outside the CNS; >90% of meningiomas are solitary (11); whereas intracranial localization of intracranial metastases [solitary intracranial dural metastases (IDM)] occurs in 8-9% of cases (12). A total of ~50% of the metastases are designated as single (located only in the CNS), and even fewer as solitary (one metastatic lesion in the whole body) (13).

It is usually safer to confidently assume a diagnosis of meningioma, even with routine magnetic resonance imaging (MRI). In the majority of cases, the task of distinguishing metastases from other types of tumors is typically straightforward. Both diagnoses are not uncommon in adult patients and, as a rule, every clinician/radiologist is familiar with typical MRI findings. Despite this, in the practice of an experienced physician, there is occasionally a situation where the differential diagnosis between these tumors is ambiguous, as intracranial meningiomas and IDM may have similar imaging characteristics; namely, a cavity-less solid structure, limited diffusion of water molecules, and the presence of extensive peritumoral edema. The variety of sources of metastases determines the variability of the cellular composition and radiological manifestations of the tumor lesion, therefore, the absence of characteristic of meningiomas (calcifications, 'spoke wheel', enostotic spine, and 'dural tail') or metastasis (necrosis cavity, hemorrhages, and large vessels) does not allow to reliably exclude one option or the other (12,14).

In addition, a number of neoplastic lesions of the meninges other than intracranial IDM such as mesenchymal tumors [solitary fibrous tumors, hemangiopericytoma, smooth muscle tumors (leiomyoma and leiomyosarcoma), epithelioid hemangioendothelioma (EH), and peripheral primitive neuroectodermal tumor-Ewing sarcoma (pPNET-ES)], intradural chordoma, leptomeningeal medulloblastoma, melanocytic tumors, and hemangioblastoma may mimic meningioma radiologically and even show the characteristic 'dural tail' of this tumor (15,16). The clinical features of some of these tumors in terms of age and sex distribution can be misleading in making a diagnosis of meningioma. For example, EH is a rare vascular soft tissue tumor with biological behavior intermediate between malignant angiosarcoma and benign angioma. CNS involvement is rare, with a total of 37 cases described in the literature. Unlike soft tissue EH, intracranial EH affects young children. Intracranial EH may present as an extra-axial meningeal lesion showing a cystic appearance and contrast enhancement on MRI, which may mimic a meningioma (15,17,18). Or a tumor such as meningeal melanocytoma, which is a low-grade solitary benign tumor that occurs at any age from 9 to 73 years, but most often in the fifth decade with a slight female predominance. On MRI, a melanocytoma appears as a well-circumscribed, hyperintense extra-axial mass with homogeneous contrast enhancement mimicking a meningioma. Therefore, although MRI is an integral part of the diagnosis of CNS tumors, histological examination of the tumor is of fundamental importance for confirming or refuting the diagnosis of meningioma. However, some of them also histologically resemble the various histotypes of meningiomas (15,19).

Since at the stage of differential diagnosis, the clinician/radiologist may not always have comprehensive data on the anamnesis of the disease (moreover, in 10% of cases in patients with brain metastases, the primary tumor was not detected at the time of presentation) (9) and/or previous studies, in the present study, it was attempted to identify

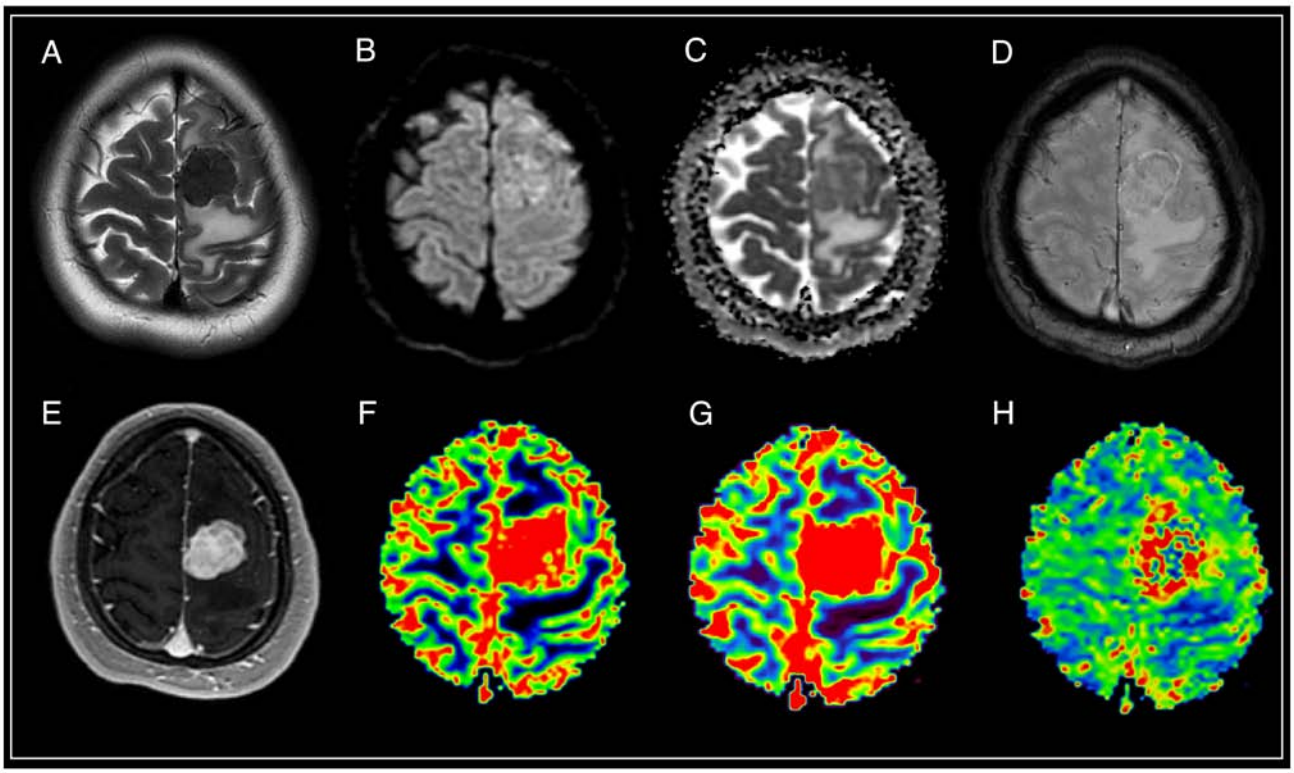

Figure 1. Brain magnetic resonance imaging of a patient with meningothelial meningioma (WHO Grade 1). Supratentorially, in the left hemisphere of the frontal region, against the background of moderate vasogenic edema, a clearly demarcated extracerebral mass is visible, characterized by a hypointense signal on T2-WI, intense and homogeneous accumulation of a contrast agent, diffusion restriction with corresponding areas of increased values of volumetric and velocity cerebral blood flow, as well as prolongation of blood transit time. SWAN indicates the presence of cortical draining veins in the formation structure. (A) T2-WI; (B and C) DWI and ADC; (D) SWAN; (E) T1-WI with contrast; (F) CBV; (G) CBF; and (H) MTT. SWAN, susceptibility-weighted angiography; T1-WI, T1-weighted image; T2-WI, T2-weighted image; DWI, diffusion-weighted imaging; ADC, apparent diffusion coefficient; CBV, cerebral blood volume; CBF, cerebral blood flow; MTT, mean transit time.

reliable criteria for distinguishing between intracranial meningiomas and IDM with similar radiological presentations using multiparametric MRI (mpMRI).

Materials and methods

Patients. The present study was approved by the Local Ethical Committee of the Federal Center of Neurosurgery (Tyumen, Russian Federation). Written informed consent for diagnostic analysis was obtained from all patients. The total number of patients was 100 (50 patients with intracranial meningiomas and 50 patients with IDM). The age of the patients ranged from 32-82 years and the median was 58 years [Note: The value of age in the present study can help in the differential diagnosis (see in Introduction), and therefore only this parameter is indicated for patients in this study, and other parameters may not affect performance].

Among the patients diagnosed with meningioma, the most common histological subtype was meningothelial meningioma, WHO Grade 1; 50% (n=25). The second most common subtype was mixed meningioma, WHO Grade 1-24% (n=12). Atypical form (WHO Grade 2) was diagnosed in 20% (n=10) of patients. In 4% (n=2) and 2% (n=1) of cases, psammomatous and secretory forms of meningiomas were identified (WHO Grade 2). The sex distribution of patients with meningiomas was 76.5% (n=38) female and 23.5% (n=12) male [Note: The value of sex in this study can help in the differential diagnosis (see in Introduction), and therefore only this parameter is indicated for patients in this study, and other parameters may not affect performance].

The group of patients with IDM from primary foci of different localization was 50 patients. Metastases with a primary focus from the breast were diagnosed in 38% (n=19) of patients, from the lungs in 34% (n=17), from the kidneys in 12% (n=6), from the prostate in 10% (n=5), and the remaining metastases, 6% (n=3), from the ovaries and large intestine. The sex of patients diagnosed with IDM was 58% (n=29) female and 42% (n=21) male. Examples of MRIs of patients with intracranial meningiomas and patients with IDM are shown in Figs. 1-4.

Execution protocol. MRI was performed using a General Electric 3T Discovery W750 tomography with an 8-channel head coil (GE Healthcare). Paramagnetic Clariscan (GE Healthcare) was used as a contrast agent with a dose calculation of 0.2 ml/kg (0.1 mmol/kg). The introduction of a contrast agent was performed in two stages: A primary dose of 0.1 mmol/kg and an additional dose of 0.2 mmol/kg. The contrast agent was injected into the cubital vein using an automatic injector at an injection rate of 5 ml/sec.

The MRI study protocol included the following pulse sequences: T1 GRE 'BRAVO', T1 SE CUBE, T2 SE, SWAN, DWI with ADC mapping, PWI-DSC-T2* (dynamic susceptibility contrast DSC-T2*).

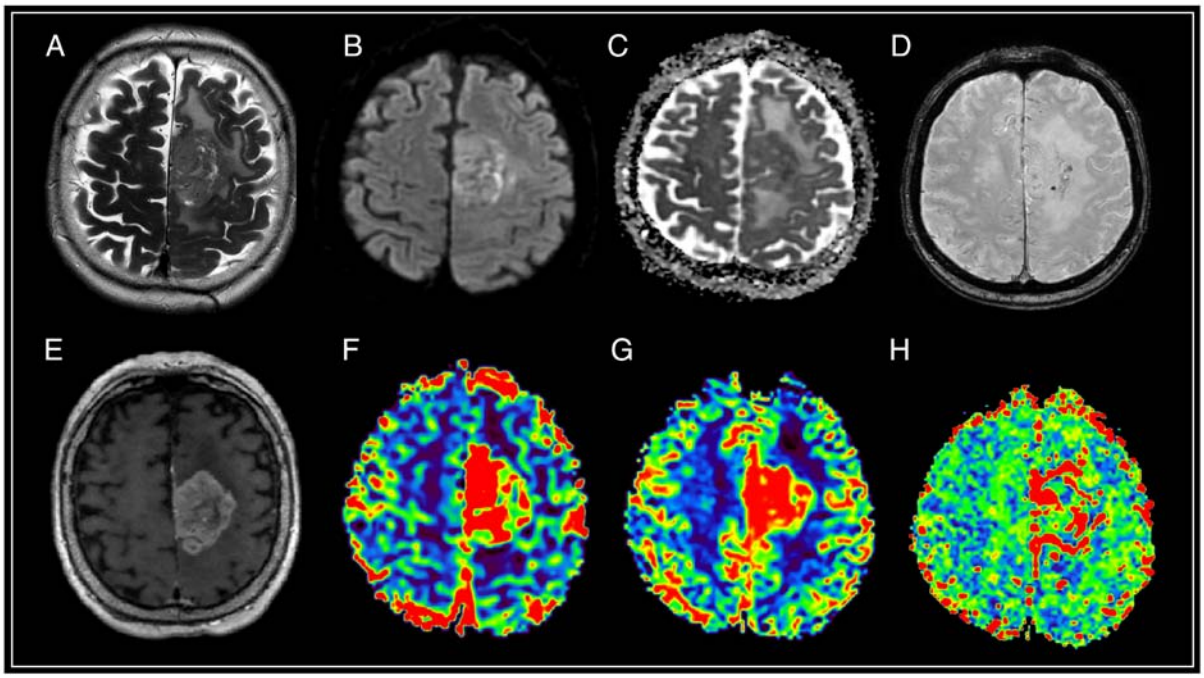

Figure 2. Brain magnetic resonance imaging with solitary intracranial dural metastasis of lung adenocarcinoma. In the parasagittal parts of the left frontal area, there is an extracerebral mass with a base on the falciform process of the dura mater, surrounded by a moderately pronounced zone of perifocal edema, relatively homogeneously accumulating contrast throughout the volume, with limited diffusion according to DWI and ADC, the presence of artifacts from blood decay products in the tumor structure, as well as high values of rCBV and rCBF, and lengthening of MTT. (A) T2-WI; (B and C) DWI and ADC; (D) SWAN; (E) T1-WI with contrast; (F) CBV; (G) CBF; and (H) MTT. SWAN, susceptibility-weighted angiography; T1-WI, T1-weighted image; T2-WI, T2-weighted image; DWI, diffusion-weighted imaging; ADC, apparent diffusion coefficient; CBV, cerebral blood volume; CBF, cerebral blood flow; r, relative; MTT, mean transit time.

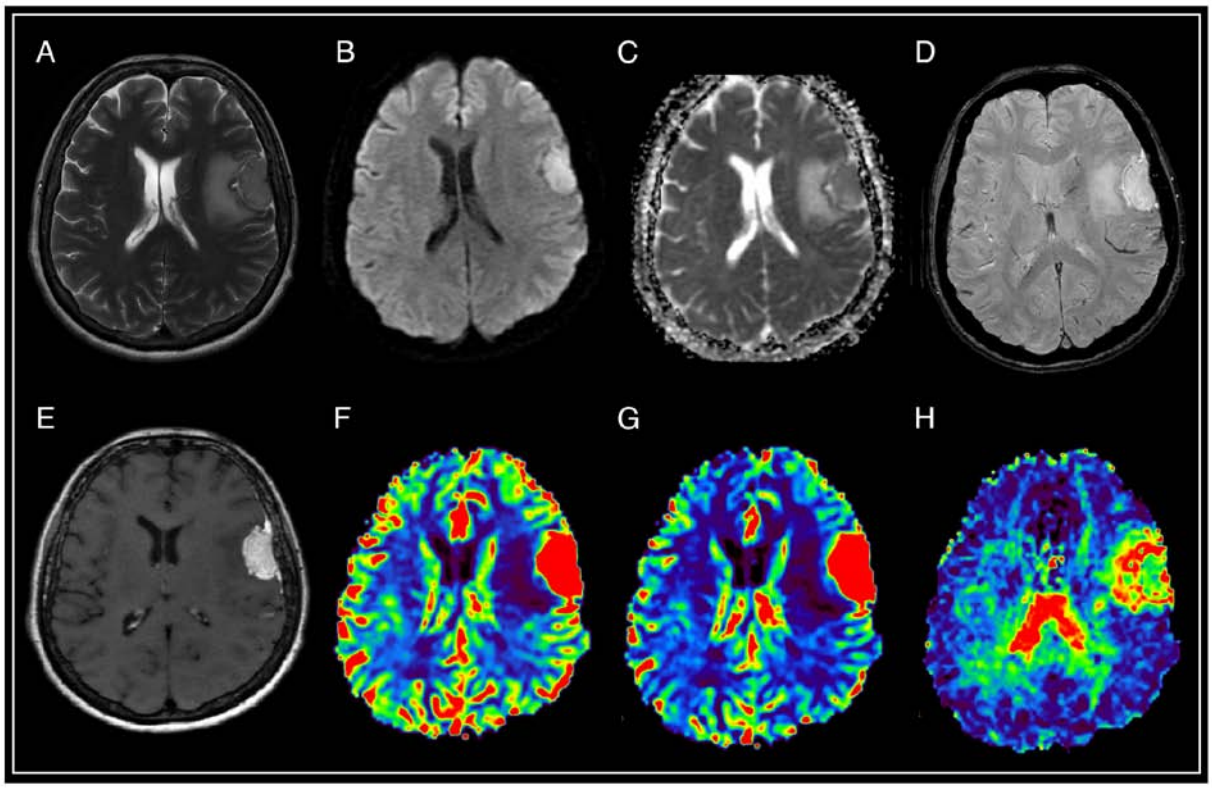

Figure 3. Brain magnetic resonance imaging of a patient with atypical meningioma (WHO Grade 2). In the frontal region of the left hemisphere, against the background of perifocal edema, an extracerebral tumor is visible with an intense and homogeneous accumulation of a contrast agent, the 'dural tail' phenomenon, diffusion limitation, an increase in volumetric and velocity cerebral blood flow, and a prolongation of blood transit time. The SWAN demonstrates the presence of peripheral draining veins around the mass. (A) T2-WI; (B and C) DWI and ADC; (D) SWAN; (E) T1-WI with contrast; (F) CBV; (G) CBF; and (H) MTT. SWAN, susceptibility-weighted angiography; T1-WI, T1-weighted image; T2-WI, T2-weighted image; DWI, diffusion-weighted imaging; ADC, apparent diffusion coefficient; CBV, cerebral blood volume; CBF, cerebral blood flow; MTT, mean transit time.

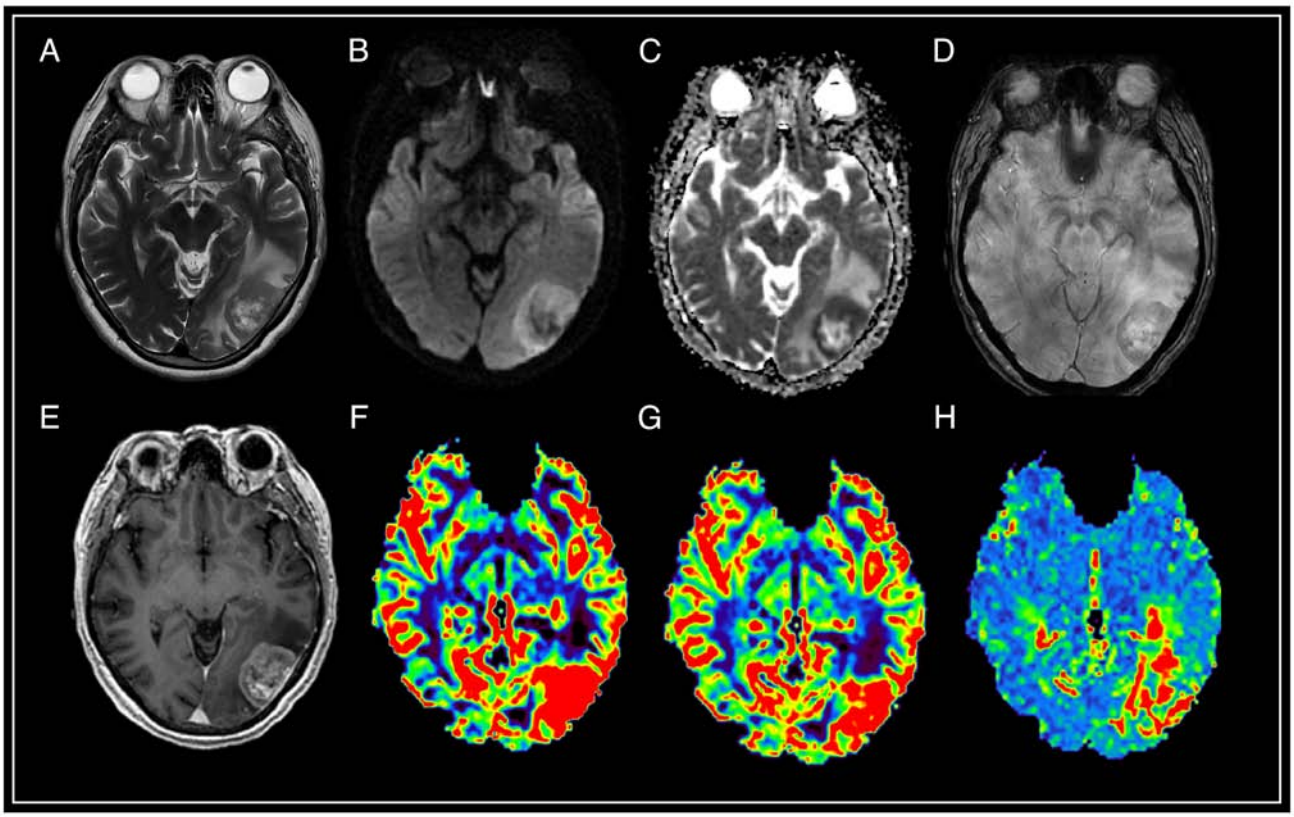

Figure 4. Brain magnetic resonance imaging with solitary intracranial dural metastasis of prostate adenocarcinoma. In the occipital region of the left hemisphere, an extracerebral formation is visible with heterogeneous contrast enhancement, and restriction of diffusion, surrounded by a pronounced zone of edema. SWAN indicates the presence of point artifacts of magnetic susceptibility due to hemorrhages and intratumoral vascular shunts. According to the results of MRI perfusion, high values of relative cerebral blood volume (rCBV) and relative cerebral blood flow (rCBF) in the tumor structure are determined. The mean transit time (MTT) indicator is extended. (A) T2-WI; (B and C) DWI and ADC; (D) SWAN; (E) T1-WI with contrast; (F) CBV; (G) CBF; and (H) MTT. SWAN, susceptibility-weighted angiography; T1-WI, T1-weighted image; T2-WI, T2-weighted image; DWI, diffusion-weighted imaging; ADC, apparent diffusion coefficient; CBV, cerebral blood volume; CBV, cerebral blood flow; r, relative; MTT, mean transit time.

Image post-processing was performed on a GE Advantage Window 4.5 graphics station (GE Healthcare). Blood flow parameters were assessed using three perfusion maps: Cerebral blood flow (CBF) in ml/100 g/min; cerebral blood volume (CBV) in ml/100 g; and mean transit time (MTT) in sec. The region of interest (ROI) in the intact white matter of the semioval centers was used to normalize blood flow parameters. The normalized blood flow parameters were calculated as the ratio of the parameter values in the area of interest to the intact brain substance, that is the relative (r)CBF and rCBV. Given the similar imaging characteristics of meningiomas with metastatic lesions, a detailed comparative analysis of all tumors was performed using both routine and specialized MRI sequences: Perfusion-weighted imaging (PWI), diffusion-weighted imaging (DWI), apparent diffusion coefficient (ADC) and susceptibility-weighted angiography (SWAN).

Data verification. The obtained data were verified using histological and immunohistochemical (IHC) analysis as follows: i) Neutral buffered formalin (10%) was used for fixation (24 h in room temperature) and in frozen sections, cold acetone was used for 1 min; ii) Paraffin embedding (mostly 4 μm) and frozen sections ranged between 4-6 μm in thickness. The IHC analysis included routine staining with both Carazzi's hematoxylin and eosin alcohol solution at room temperature (~24˚C) for 15 min. The range of IHC markers used were as follows: 7 ml Anti-EMA (E29) (cat. no. Z2048MP; Thermo Fisher Scientific, Inc.), 500 μl Ki-67 (SP6) (cat. no. PIMA514520; Invitrogen™; Thermo Fisher Scientific, Inc.), 7 ml Cytokeratin Cocktail (AE1 & AE3) (cat. no. MBS370057; MyBioSource, Inc.), and 100 μg/vial Anti-Vimentin (v9) (cat. no. MA1102; Boster Biological Technology). Incubation Time/Temperature of IHC markers: Anti-EMA (E29) 1-3 min/room temperature; Ki-67 (SP6) 30-60 min/room temperature; Cytokeratin Cocktail (AE1 & AE3) 15 min/room temperature; and Anti-Vimentin (v9) 5-10 min/room temperature. Cells were counted using an Aperio ImageScope 12.4.6-Pathology Slide Viewing Software using the nuclear, cytoplasmic, and membrane staining module in the Aperio Image Analysis Workstation.

CBV and CBF characteristics. CBV and CBF in high-grade intracranial meningiomas and intracranial metastases show a high degree of heterogeneity. Low and high CBV and CBF threshold values may be the result of various pathological features. Therefore, to characterize the tumor, it is necessary to stratify the CBV/CBF into low and high regions. When choosing the thresholds, the following three facts were taken into account: i) Normal brain tissue has intrinsic differences depending on tissue type as CBV and CBF are greater in gray matter than in white matter, and even higher in large vessels; ii) some tumor vessels may originate from cerebral vessels;

and iii) several studies have that the distribution of CBV in the tumor is more or less similar to that in normal tissue, although the vasculature of intracranial meningiomas and IDM has morphological and functional abnormalities (20-22). Thus, instead of choosing arbitrary threshold values, the CBV and CBF values in normal gray and white matter reported in published studies to were used divide tumor perfusion into regions of high, medium, and low levels (23,24). The area of high CBF was defined as >120 ml/100 g/min. Similarly, the lower region was defined as less than 50 ml/100 g/min but >10 ml/100 g/min. A lower threshold value of 10 ml/100 g/min was used to exclude voxels that could represent a surgical cavity or necrosis. Similarly, CBV threshold values were divided into three groups: High CBV, >4%; average CBV, 1.7-4%; and low CBV, 0.2-1.7%.

Statistical analysis. Statistical processing of the obtained results was performed using descriptive statistics and correlation analysis. Sex, age, presence of dislocation of midline structures, bone invasion, and severity of perifocal edema were compared for both groups of patients using a Pearson's χ^2 test or ANOVA as appropriate. ADC, CBV, rCBV, CBF, rCBF, and MTT values were compared for both groups of patients using a Mann-Whitney U test. The optimal cut-off value, which can provide the sensitivity and specificity needed to differentiate meningioma from dura metastases, was determined by analysis of ROC curves. The area under the ROC-curve values (AUC) was calculated for the CBV, rCBV, CBF, and rCBF values. CBV, rCBV, CBF, and rCBF value parameters were analyzed on the MRI software SPHERE® version 3.0. Statistical analyses were performed using IBM SPSS version 24.0 software (IBM Corp.), and the graphs were generated using GraphPad Prism version 8.0 (GraphPad Software, Inc.). P<0.05 was considered to indicate a statistically significant difference.

Results

Neuroimaging data. The results indicated that IDM affected bone less frequently (P≤0.001) than intracranial meningiomas; bone invasion by metastasis was observed in only 2% (n=1) of cases (Fig. 5A).

In addition, dislocation of the midbrain structures in patients with meningiomas was observed in 12% of cases (n=6), and in patients with IDM in 22% of cases (n=11). There were no significant differences in dislocation between the different groups of patients (P=0.169). In 60% of cases (n=30) there was no perifocal edema in the meningioma patient group, whereas in 40% of perifocal edema cases was detected; 20% (n=10) of mild severity and 20% (n=10) of moderate severity. Moreover, perifocal edema in the group of patients with IDM was significantly more common (P≤0.001) compared with patients with meningioma, where 48% of patients (n=24) had moderate and severe edema, 42% (n=21) had mild edema, and 10% (n=5) was absent (Fig. 5B).

In the group of intracranial meningiomas, the mean ± SD ADC was $912.14x10^{-6}$±$102.7x10^{-6}$ mm^2/sec. The median CBV was 19.25 ml/100 g (CI, 18.08-28.96 ml/100 g) and the median increase in rCBV was 4.1-fold (CI, 4.09-5.46). The median CBF was 155 ml/100 g/min (CI, 157.48-206.65 ml/100 g/min)

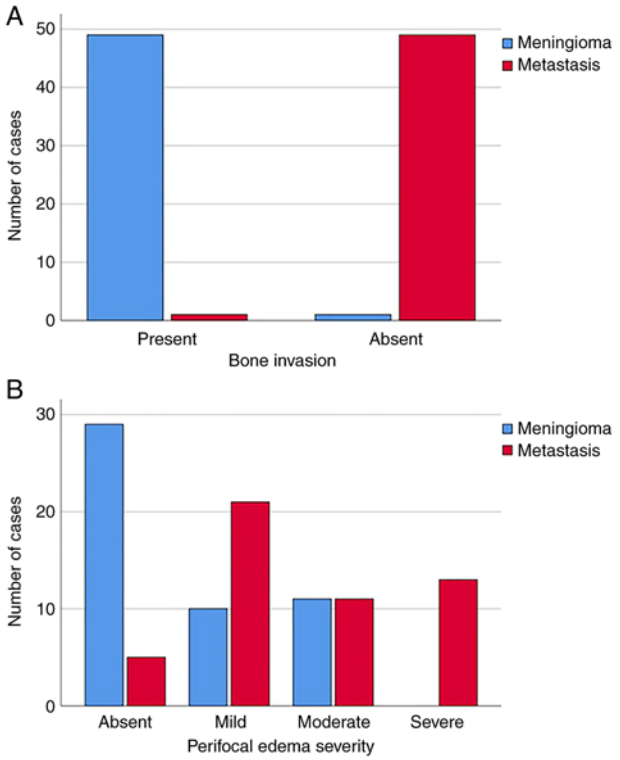

Figure 5. Comparison of some characteristics of patients with intracranial meningiomas and solitary IDM. The incidence of (A) bone invasion and (B) the severity of perifocal edema among patients with intracranial meningiomas and solitary IDM. The prevalence of bone invasion was shown grater in cases with meningiomas than in cases with IDM (P<0.001), as well as a greater severity of perifocal edema in patients with metastases (P<0.001). IDM, intracranial dural metastasis.

and the median increase in rCBF was 3.85-fold (CI, 3.98-5.28). The median MTT was 11 sec (CI, 10.18-11.29 sec).

In the IDM group, the mean ± SD ADC was $867.67x10^{-6}$±$138.6x10^{-6}$ mm^2/sec. The median CBV was 39.85 ml/100 g (CI, 36.50-46.83 ml/100 g) and the median increase in rCBV was 7.15-fold (CI, 6.64-7.80). The median CBF was 293 ml/100 g/min (CI, 261.65-306.12 ml/100 g/min) and the median increase in rCBF was 6.7-fold (CI, 5.97-6.93). The median MTT was 10.85 sec (CI, 10.15-10.86 sec).

According to the results of the comparative analysis, a statistically significant difference in the values of the CBV, rCBV, CBF, and rCBF indicators was revealed. In the IDM group, perfusion values were significantly higher (P≤0.001). There were no differences between ADC and MTT (P=0.071 and P=0.127, respectively) in IDM and meningioma patient groups. The results of the comparisons are shown in Table I and Fig. 6.

Diagnostic value. Determination of perfusion threshold values (for indicators with significant differences-CBV, rCBV, CBF, and rCBF) for differentiating intracranial meningiomas and IDM was performed by constructing ROC curves and calculating the optimal sensitivity and specificity values (Fig. 7). The threshold value for CBV was 28.25 ml/100 g; the sensitivity and specificity were 76.5 and 78.0%, respectively (Fig. 7A). The threshold value for rCBV was 5.4; The sensitivity and specificity of the method are 74.5 and 82.0%, respectively

Table I. Average ADC, MTT, averaged absolute BF and BV, and BFn and BVn in tumors based on the histological affiliation.

Significative	Intracranial meningioma	Intracranial dural metastases	P-value
ADC, x10^{-6} mm^2/sec	912.14 (SD: ±102,7)	867.67 (SD: ±138,6)	0.071
BV, ml/100 g	19.25 (CI: 18,08-28,96)	39.85 (CI: 36,50-46,83)	<0.001
BVn	4.1 (CI: 4,09-5,46)	7.15 (CI: 6,64-7,80)	<0.001
BF, ml/100 g/min	155.0 (CI: 157,48-206,65)	293.0 (CI: 261,65-306,12)	<0.001
BFn	3.85 (CI: 3,98-5,28)	6.7 (CI: 5,97-6,93)	<0.001
MTT, sec	11 (CI: 10,18-11,29)	10.85 (CI: 10,15-10,86)	0.127

ADC, apparent diffusion coefficient; MTT, mean transit time; BF, blood flow; BV, blood volume; n, normalized.

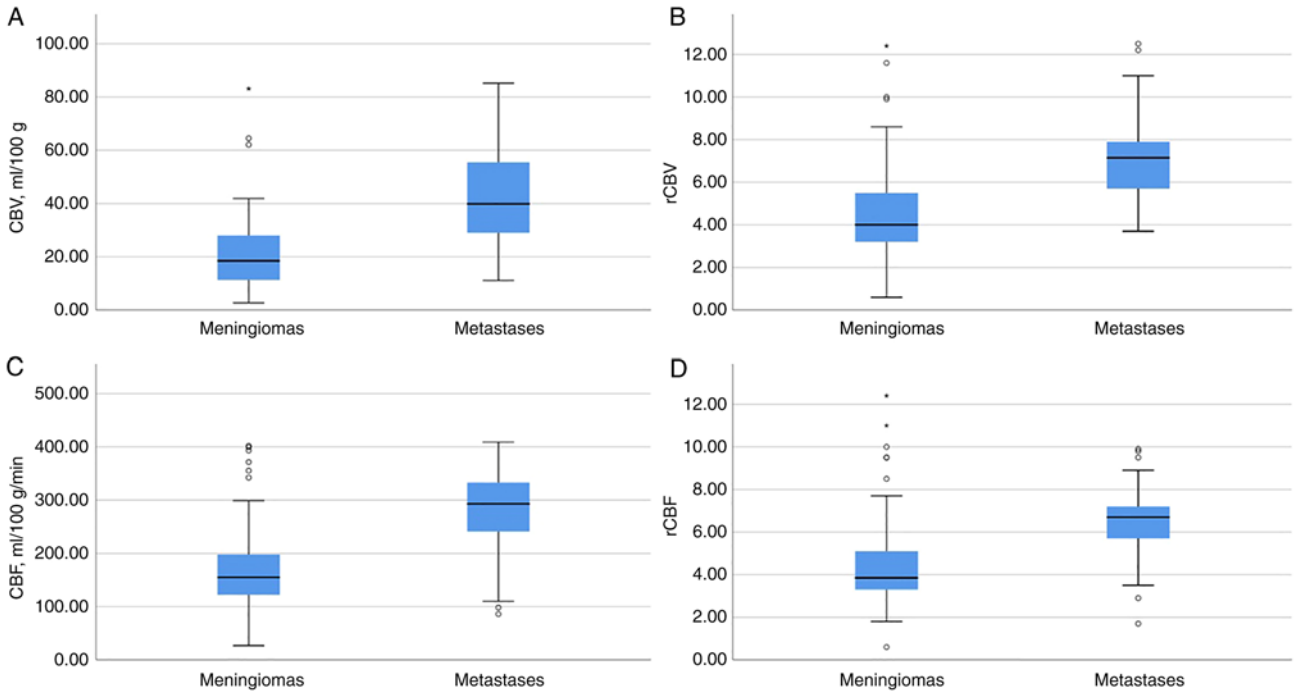

Figure 6. Demonstration of evaluating the results of the values of the CBV, rCBV, CBF, and rCBF. Graphs of (A) CBV, (B) normalized rCBV, (C) CBF velocity, and (D) normalized rCBF velocity for intracranial meningiomas and solitary IDM. (A) The median CBV was significantly higher for IDM than for intracranial meningiomas (P≤0.001). The Y-axis plots the values of the CBV in ml/100 ml; (B) the median increase in rCBV was significantly higher for IDM than for intracranial meningiomas (P≤0.001). The Y-axis plots the ratio of rCBV in the ROI to the normal white matter of the semioval center, representing the normalized cerebral blood flow volume; (C) Median CBF was significantly higher for IDM than for intracranial meningiomas (P≤0.001). The Y-axis shows the values of CBF velocity in ml/100 g/min. (D) The median rCBF was significantly higher for IDM than for intracranial meningiomas (P≤0.001). The Y-axis plots the ratio of rCBF velocity in the ROI to the normal white matter of the semioval center, representing the normalized rCBF velocity. ROI, region of interest; IDM, intracranial dural metastasis; CBV, cerebral blood volume; CBV, cerebral blood flow; r, relative.

(Fig. 7B). The threshold value for CBF was 217.9 ml/100 g/min; the sensitivity and specificity were 80.4 and 86.0%, respectively (Fig. 7C). The threshold value of the rCBF was 5.6; the sensitivity and specificity were 82.4 and 76.0%, respectively (Fig. 7D).

With the indicated threshold values of all the listed perfusion indicators ≤ threshold, it was worth considering an intracranial meningioma.

Histological and immunohistochemical methods. Examples of histological and immunohistochemical studies of a patient with atypical meningioma (WHO Grade 2) and an IDM patient with a primary focus on adenocarcinoma and clear cell renal cell carcinoma are shown in Figs. 8-11.

Discussion

The most common meningeal tumor is meningioma, which is regularly diagnosed through MRI scans as incidental findings. Most meningiomas are histologically and biologically benign, characterized by non-aggressive, very slow growth, and a low risk of recurrence (WHO Grade 1). Small meningiomas are clinically asymptomatic. At the same time, large tumors and tumors with perifocal edema have a mass effect with the manifestation of a variety of neurological symptoms, in particular cerebral (headaches) and focal (paresis).

Data from the largest single-center study, which included 1,000 cases from between 2004 and 2010, showed that 2% of resected dural masses, initially regarded radiologically

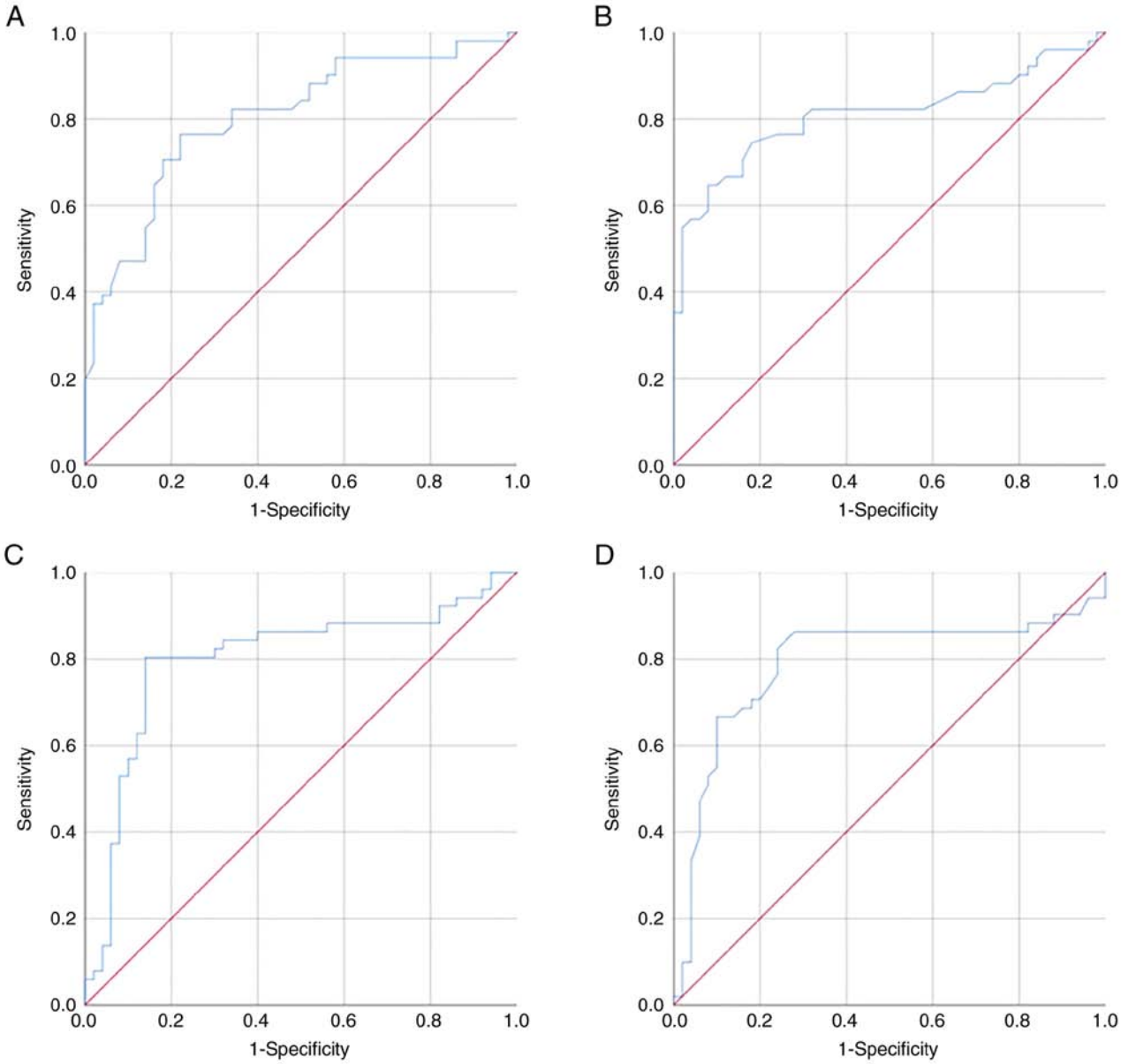

Figure 7. The ROC curve and the AUC analysis. (A) The AUC corresponding to CBV for differentiating intracranial meningiomas and solitary IDM was 0.805±0.44 [95% CI, 0.719-0.890] (P≤0.001) with sensitivity and specificity values of 76.5 and 78.0%, respectively; (B) The AUC corresponding to rCBV for differentiating intracranial meningiomas and IDM was 0.811±0.46 [95% CI, 0.722-0.900] (P≤0.001) with sensitivity and specificity values of 74.5 and 82.0%, respectively. (C) The AUC corresponding to CBF for differentiating intracranial meningiomas and IDM was 0.8±0.48 [95% CI, 0.706-0.894] (P<0.001) with sensitivity and specificity values of 80.4 and 86.0%, respectively. (D) The AUC corresponding to rCBF for differentiating intracranial meningiomas and IDM was 0.79±0.5 [95% CI, 0.692-0.888] (P≤0.001) with sensitivity and specificity values of 82.4 and 76.0%, respectively. If the values of CBV, rCBV, CBF, and rCBF were ≤ threshold value, the patient was predicted to have an intracranial meningioma. The threshold value of CBV was 28.25 ml/100 g, for rCBV it was 5.4, for CBF it was 217.9 ml/100 g/min, and for rCBF was 5.6. ROC, receiver operating characteristic; AUC, area under the curve; IDM, intracranial dural metastasis; CBV, cerebral blood volume; CBV, cerebral blood flow; r, relative.

and intraoperatively as meningiomas, were, in fact, mimic pathologies, amongst which the largest number were metastases (25). The exact incidence of IDM is difficult to estimate. Carcinomatous infiltration of the dura mater is detected in patients with primary extraneural malignancies in 8-9% of cases and usually as a late manifestation (12). In ~20% of IDM cases, there are no symptoms. Otherwise, the most common clinical manifestations are symptoms of increased intracranial pressure, neurological deficits, and seizures (12).

As a rule, the differential diagnosis of meningioma and CNS metastases does not cause difficulties for a neuromorphologist. In rare cases, at the initial stage of microscopic examination of histological slides stained with hematoxylin and eosin, a clear picture may not immediately emerge (Figs. 10 and 11). On such occasions, the pathologist should use IHC to determine the histogenesis of the tumor.

From a radiological point of view, a typical meningioma and a typical metastasis appear notably different in routine MRI examination. Benign meningiomas are close to spherical or plaque-shaped, creeping along the dura matter configuration. Often, meningiomas are delineated from the brain parenchyma by a cerebrospinal fluid cleft, sometimes containing depressed extracerebral vessels. Characteristic of meningiomas is the presence of almost always vivid and homogeneous contrast

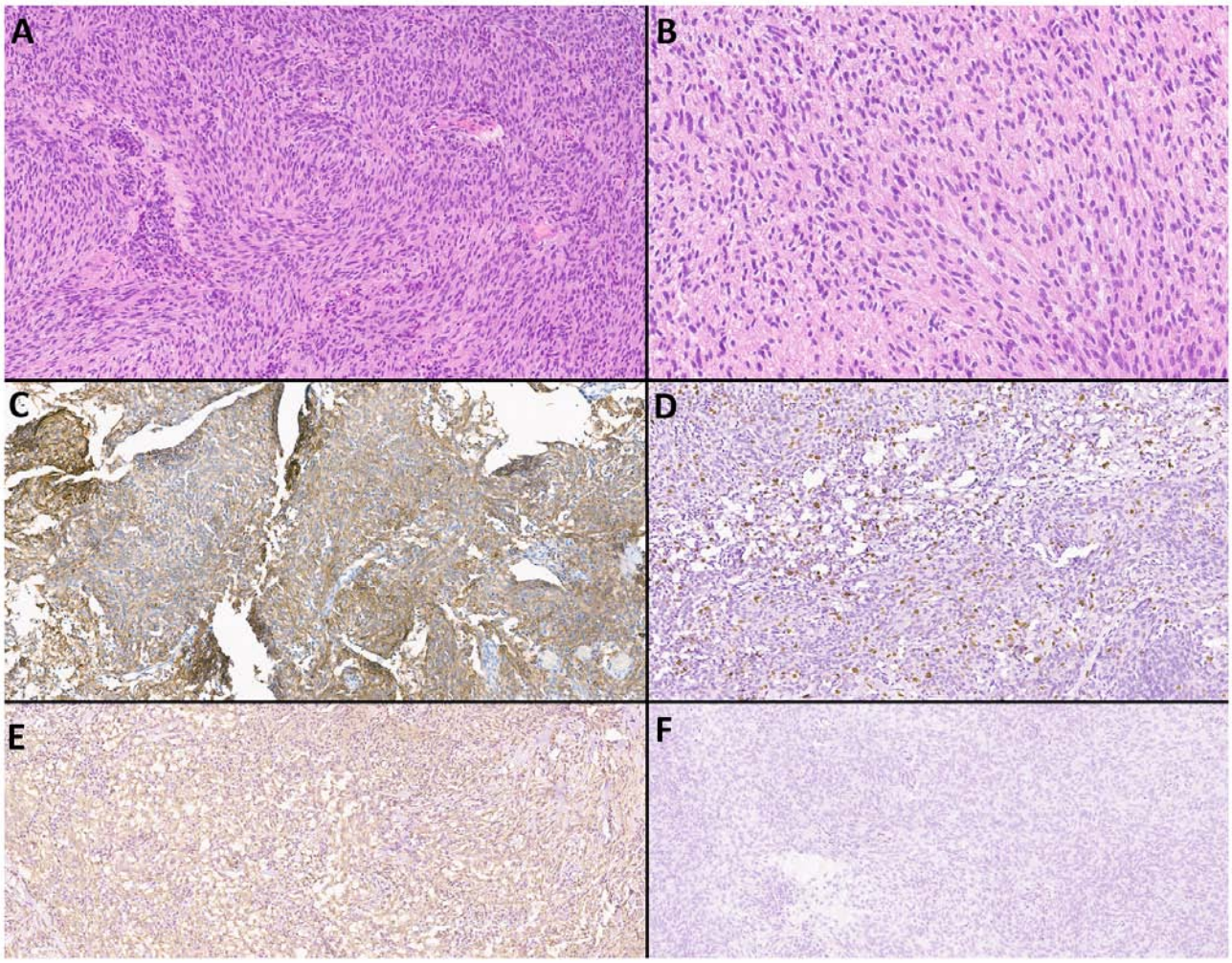

Figure 8. Patient with atypical meningioma (WHO Grade 2). (A and B) Examination of a series of prepared slides stained with hematoxylin and eosin reveals tumor tissues built from arachnoid endothelial cells. Cellularity was increased. The nuclei were predominantly round-oval or slightly elongated with a small centrally located nucleolus. The cytoplasm varies in tinctorial properties from optically transparent to light oxyphilic. The cells were located in continuous fields with the formation of multidirectional vortices. In most cellular zones, there were mitotic figures up to 4-5 figures/10 points (magnification, x40). The stroma was unevenly expressed and rich in collagen. On immunohistochemical examination, tumor cells expressed (C) Vimentin, (D) with a Ki-67 proliferation index of 10%, (E) non-uniformly diffusely anti-EMA, or (F) complete absence of pankeratin AE1/AE3.

enhancement, accompanied by non-pathognomonic reactive thickening of the dura in the form of a 'dural tail', visible in 60-72% of cases (25). Additionally, ~25% of meningiomas contain calcifications, the presence of which is associated with a slow growth rate and a low degree of malignancy (26). Hemorrhages are not characteristic of meningiomas. In 20% of cases, the bone bearing the base of the meningioma shows focal reactive hyperostosis in the form of a spike (27). Since the center of the meningioma is supplied with blood through the stalk at the point of attachment to the dura matter from the branches of the external carotid artery (for example, from the middle meningeal artery), the supplying artery 'radiates' from one point to the periphery of the tumor, appearing as 'sun rays' or a 'spoked wheel' on T2-WI and on postcontrast T1-WI. Meningiomas can grow into the adjacent bone and even the scalp, into the lumen of the dural sinus, or envelop nerves and arteries, typically causing stenosis of the latter. Of note, >50% of meningiomas have peritumoral vasogenic edema (28). On DWI, meningiomas appear as tumors with high cellularity as they show a high signal corresponding with low ADC values. It is hypothesized that malignant meningiomas have lower ADC values; however, benign meningiomas can also have similar diffusion index numbers, which creates confusion (29).

Meningiomas are highly vascularized tumors. Surgical resection of a meningioma carries a high risk of blood loss (30). In PWI, meningiomas show elevated rCBV values, which vary slightly based on the specific histological subtype (31).

Intra-axial metastases, in the vast majority of cases, are easily distinguishable from meningiomas according to mpMRI, and have a number of typical imaging characteristics. Metastases, as a rule, are typically located at the border of the gray-white matter and in the border zones between the territories of the arterial pools, accompanied by variably pronounced vasogenic edema. For metastasis, a ring-shaped contrast enhancement pattern is typical with a central area of necrosis and hemorrhages. Average ADC values are within $919.4\pm200x10^{-6}$ mm^2/sec. Increased perfusion values along the periphery of the formation are characteristic (32). According to previous studies, IDM may look identical to intracranial

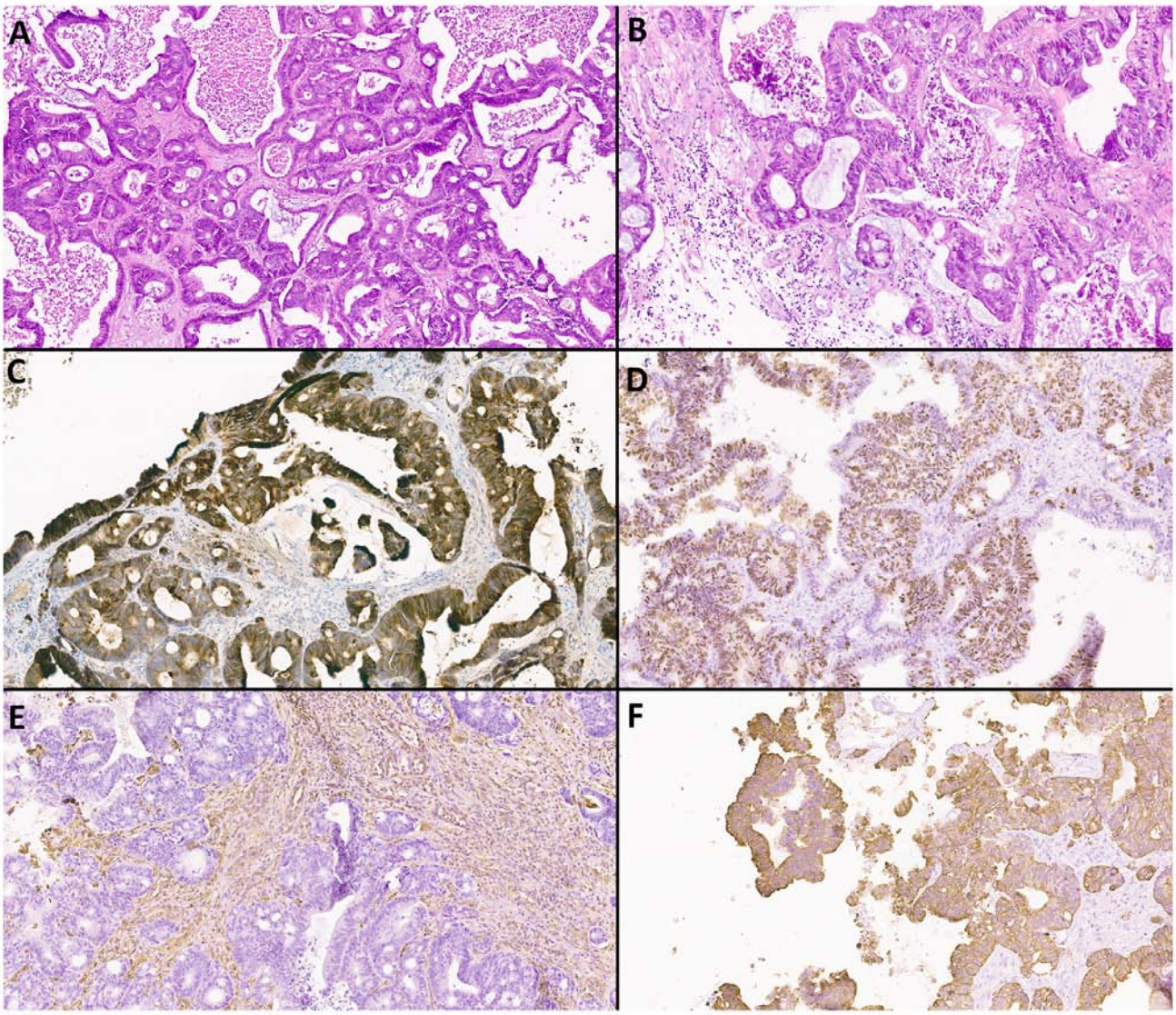

Figure 9. A patient with metastatic adenocarcinoma of the sigmoid colon. (A and B) When examining a series of prepared slides stained with hematoxylin and eosin, tumor tissue was determined based on the presence of atypical epithelial cells with manifestations of pronounced nuclear polymorphisms. The nuclear-cytoplasmic ratio was increased. The chromatin pattern was heterogeneous and smeared. There were numerous pathological mitoses, 1-2 figures in each field of view (magnification x40). Cells form cribriform and tubular glandular structures. Stroma with myxoid changes, poorly expressed, exhibited infiltration of small lymphocytes, and extensive necrosis in all fields of vision. (C) Tumor cells were strongly stained with anti-EMA, (D) Ki-67 proliferative activity index of 50%, (E) Vimentin expression in the stromal component, and (F) pankeratin AE1/AE3.

meningiomas, and any meningeal lesion is subject to a differential diagnosis (33,34).

IDM typically presents as a focal nodular dural thickening accompanied by perifocal vasogenic edema of variable severity unrelated to the size of the lesion. Extensive edema has a mass effect, compressing the brain parenchyma (35). In rare cases, swelling may be absent. Post-contrast IDM series show intense accumulation of the paramagnet. In half of the cases, the phenomenon of the 'dural tail' occurs, sometimes hemorrhages are observed in the structure of the tumor. A number of authors have hypothesized that IDM is more likely to exhibit facilitated diffusion (12,16,36). A small number of studies have found a correlation between low ADC values and low metastatic differentiation, as well as increased cellularity (37). However, it has also been shown that there is no correlation between ADC values and the histological nature of the metastasis (38); thus, this remains a contested result. A summary and comparison of routine imaging findings are shown the Table II.

Perfusion of metastases varies depending on the nature of the primary lesion, and can be either hypo- or hypervascular. The majority of metastases, in particular those of renal carcinoma, melanoma, and neuroendocrine carcinoma, are hypervascular. According to Kremer *et al* (36). and Furtner *et al* (39), both of which had small sample sizes, IDMs were less vascularized than intracranial meningiomas. The work of Fink and Fink (40) and Bendini *et al* (41) showed that rCBF and rCBV values were similar to those of meningiomas on perfusion maps. Lui *et al* (42), did not reveal statistically significant differences in rCBV and MTT values between the study groups based on the analysis of 12 cases of intracranial meningiomas and 8 cases of IDM. A summary and comparison of advanced imaging findings are presented in Table III.

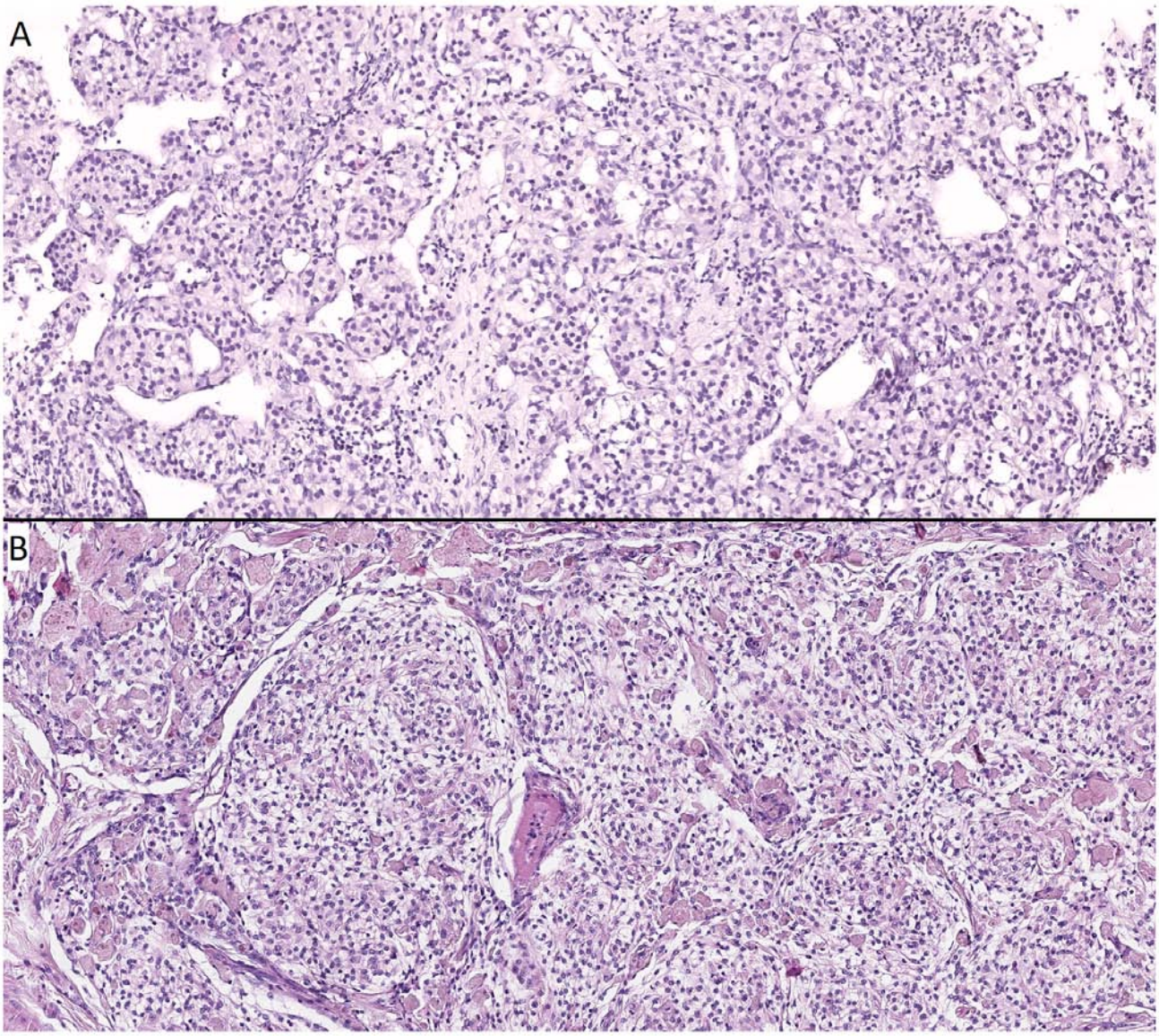

Figure 10. Microscopic examination of histological preparations from a patient with intracranial meningioma and solitary IDM (metastasis of clear cell renal cell carcinoma). (A) Hematoxylin and eosin stained clear cell renal cell carcinoma metastasis (magnification, x20). (B) Hematoxylin and eosin stained clear cell meningioma (magnification, x20). The cells possessed a similar morphology in shape and size, the cytoplasm in both cases was optically transparent, cells were located in continuous fields, and in certain regions, the stromal component outlined small lobed structures. IDM, intracranial dural metastasis.

CBV and the CBF also highlight the importance of cerebral vascular autoregulation. The CBV threshold value of angiomatous meningiomas is higher than that of meningothelial meningiomas and higher than that of fibroblastic meningiomas (36). A high CBV threshold value with swelling around the lesion is indicative of anaplastic meningioma (36). The CBV threshold value observed in the metastatic peritumoral area was lower than that observed in anaplastic meningioma due to tumor infiltration around the lesion seen in anaplastic meningioma (36,43). This CBV threshold value appears to be reliable in clinical practice for distinguishing between two tumor masses even though there is overlap. For instance, patients with high- or low-grade gliomas with a high relative rCBV (>1.75) have a significantly more rapid time to progression than patients who have high-grade gliomas and low-grade gliomas with a low relative CBV (44,45). In addition, CBV and rCBV have been shown to correlate with both catheter angiography scores of tumor hypervascularization and histopathological measurements of tumor neovascularization and mitotic activity (46). Intratumoral perfusion in intracranial meningiomas is increased with a median rCBV of 8.9 due to the increased vascularization and absence of the blood-brain barrier (BBB), while similar indicators in various intracranial IDM are only slightly increased with a median rCBV of 1.8 (24,47). However, hypervascular intracranial IDM from primary tumors such as melanoma, renal cell carcinoma, and Merkel cell carcinoma may present with an elevated rCBV indistinguishable from that of meningiomas (37,39). Hakyemez *et al* (48) demonstrated that typical meningiomas had an rCBV value of SD 6.63±2.87, whereas in atypical meningiomas it was 12.25±4.63 ($P<0.01$). The CBF of a normally perfused area is >40 ml/100 g/min, the CBF of a zone of oligemia is between 20-40 ml/100 g/min, the CBF of a zone of penumbra is between 10-20 ml/100 g/min, the CBF

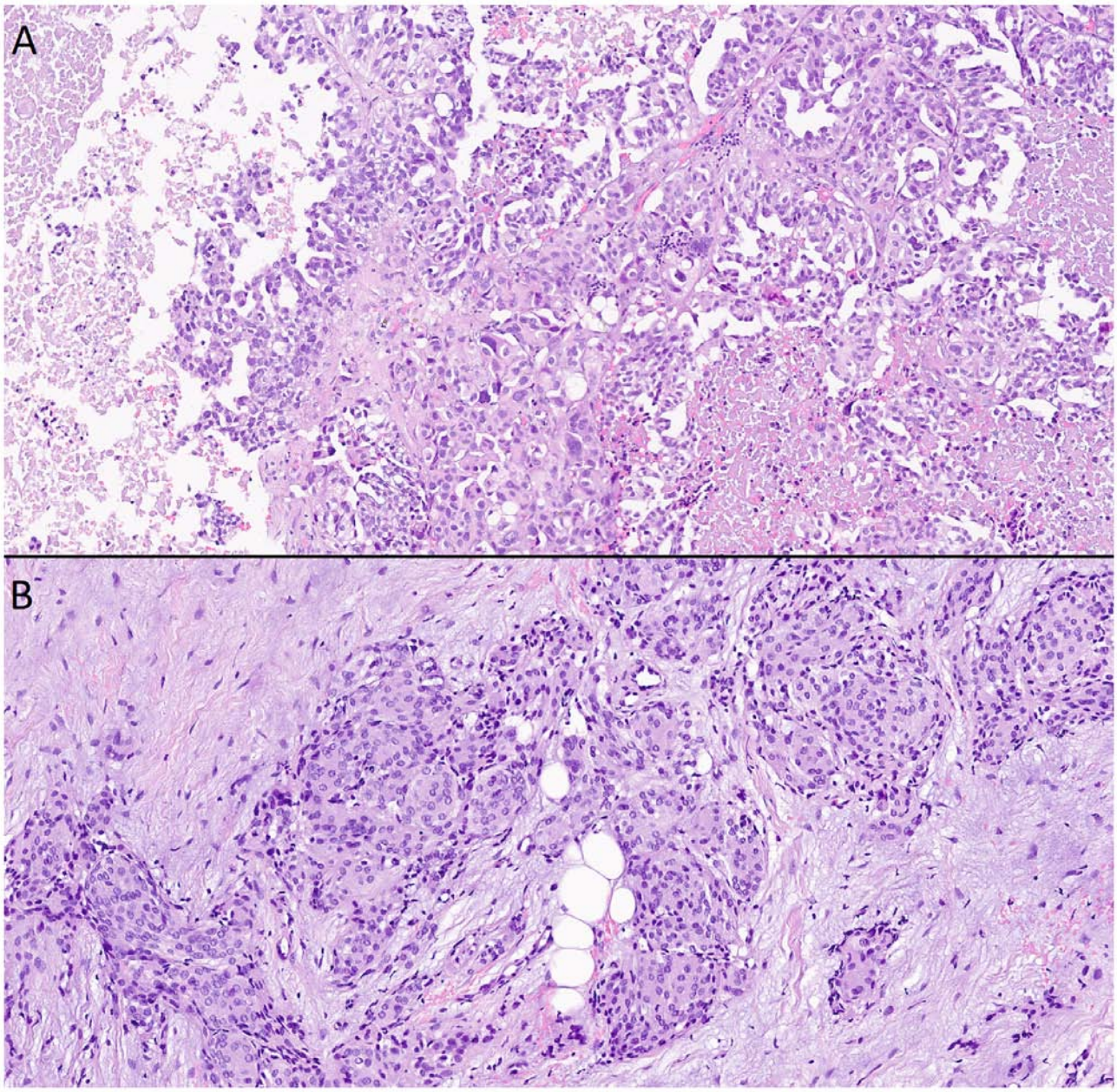

Figure 11. Microscopic examination of histological preparations from a patient with intracranial meningioma and solitary intracranial dural metastasis (metastasis of acinar adenocarcinoma of the prostate). (A) Metastasis of acinar adenocarcinoma of the prostate, stained with hematoxylin and eosin, (magnification, x20). Cells of a large size with glandular morphology, nuclei polymorphic in shape and size, with a cytoplasm that appeared outlined, optically light, varied in volume, with moderate lymphocytic infiltration, and continuous fields of necrosis on the left and right. (B) Meningothelial meningioma, stained with hematoxylin and eosin (magnification, x20). Cells were of a medium size, with a similar structure, and an arachnoid endothelial appearance, forming typical microconcentric structures; the nuclei were round-oval and monomorphic; the stroma was fibrous and well expressed.

of an ischemic zone is <10 ml/100 g/min (49). Lin *et al* (50) suggested that compared with solitary metastases, CBF values in the peritumoral edema of glioblastoma may be elevated by tumor cell angiogenesis. Based on this, it was hypothesized that the difference in CBF values from an area of edema close to an enhanced lesion to an area close to normal-looking white matter in intracranial meningiomas and IDM could be reflected as a gradient-the CBF gradient.

Despite histological and radiological differences, there are situations where meningiomas and IDMs appear similar on MRI, and the differential diagnosis between these tumors based on imaging alone is ambiguous. In addition, the medical history is not always exhaustive, and archival data may not be available, making it impossible to assess growth dynamics. Preoperative differentiation is required to determine the treatment approach: Dynamic observation, surgical resection, additional examination to search for the primary focus and staging, and the possibility of using adjuvant therapy (39,41,42,51,52). IDM, unlike parenchymal and leptomeningeal metastases, are localized outside the BBB, thus remaining susceptible to systemic chemotherapy (34). Therefore, the search for reliable radiological markers to differentiate IDM is essential in clinical practice. In such situations, the radiologist should try to increase the specificity with additional

Table II. Comparison of a meningioma, an intra-axial metastasis, and routine MRI imaging findings of IDM.

Routine imaging findings	Lesion		
	Meningioma	Intra-axial metastasis	Intracranial dural metastasis
Morphology	Close to spherical or plaque-shaped	Close to spherical	Close to spherical or focal dural thickening
CSF cleft sign	Characteristic	No CSF cleft sign	Present
Contrast enhancement characterization	Vivid and homogeneous	Vivid with ring pattern	Vivid and often homogeneous
Dural tale sign	Occurs in 60-72% of cases	No dural tale sign	Occurs in 50% of cases
Calcifications	Occurs in 25% of cases	Absent	Absent
Hemorrhages	Absent	Typical	Occurs but depends on the source of tumor nature
Focal hyperostosis	Occurs in 20% of cases	Absent	Absent
Sun rays or spoked wheel sign	Typical feature	Absent	Absent
Extracerebral vessels involvement	Arterial encasement with lumen stenosis; dural venous sinuses invasion	No extracerebral vessels involvement	Arterial encasement without lumen stenosis; no dural venous sinuses invasion
Bone invasion	Occurs without bone destruction	No bone invasion	Occurs with bone destruction
Vasogenic edema	Occurs in 50% of cases	Typical and depends of tumor origin	Typical and depends of tumor origin

IDM, intracranial dural metastases.

Table III. Comparison of a meningioma, an intra-axial metastasis, and advanced MRI imaging findings of IDM.

Routine imaging findings	Lesion		
	Meningioma	Intra-axial metastasis	IDM
Diffusion restriction	Typical and observed in entire mass	Varies and observed thenon-necrotic mass periphery	Varies and depends from the source tumor cellularity
CBV and CBF, rCBV and rCBF values	Increased in entire mass	Increased in non-necrotic mass periphery	Vary and depend from the source tumor nature

IDM, intracranial dural metastases; CBV, cerebral blood volume; CBF, cerebral blood flow; r, relative.

instruments and perform a multiparametric study, in particular DWI/ADC and PWI. According to the results of the present study, there was no statistically significant difference between the mean ADC and MTT values for meningiomas and IDM. When analyzing perfusion parameters (CBV, rCBV, CBF, and rCBF), differences were found, including results that contrasted the results reported by Kremer *et al* and Furtner *et al* namely, IDM perfusion rates were higher in patients with meningiomas. In addition, the threshold value of the CBF indicator was calculated, a value above this which makes it possible to predict IDM with sensitivity and specificity in the region of 90.0% (80.4 and 86.0%, respectively).

As it has been aforementioned, there are differences in the degree of bone invasion and surrounding edema between meningiomas and isolated intracranial IDM on MRI. Indeed, these factors undoubtedly affect the prognosis and treatment options, and again proving the importance of a correct diagnosis using one of the methods such as neuroimaging. The use of high-dose dexamethasone may produce symptomatic relief, even if there is no evidence of cerebral edema on MRI. Immediate evacuation of a subdural hematoma can be a life-saving procedure. Surgical resection is the best treatment when the lesion is unique, accessible, and circumscribed, particularly when the systemic disease

is controlled or not immediately life-threatening (53). However, even in the case of progressive systemic cancer, some surgeons recommend resection when the IDM causes severe symptoms. After total removal of the tumor, the resected dura is replaced by an artificial dura (54). In some data, surgery was performed in 83% of cases, alone or associated with another treatment. In our experience, this figure largely overestimates the number of patients eligible for surgery and is probably biased by the publication of a higher number of surgical series. Radiation therapy is indicated in patients who cannot be operated on because the IDM is inaccessible or widespread or because life expectancy due to the progression of the systemic diseases does not exceed a few months. Systemic chemotherapy was used in very few cases but could not be evaluated because of its almost constant association with surgery and/or radiotherapy. Considering that this also depends on the individuality of the case, depending also on the experience of the surgeon, the equipment of the operating room and the patient's systemic diseases (55,56).

In conclusion, diffusion-weighted images are not reliable criteria for differentiating intracranial meningiomas from IDM and should not influence the diagnosis suggested by imaging. The meningeal lesion perfusion technique predicts metastasis with a sensitivity and specificity close to 80-90% and deserves attention in the diagnosis. Since IDM differs from meningiomas in the severity of neoangiogenesis and, accordingly, in greater vascular permeability, the technique for assessing vascular permeability (wash-in parameter with dynamic contrast enhancement) may potentially be used as an additional criterion for distinguishing between dural lesions. In addition, this method has not been brought to extensive practice, thus the purpose of this study was to examine it. Since it was observed that this is possible, the next step is multicenter prospective randomized trials on this topic.

Acknowledgements

Not applicable.

Funding

The present study was supported by the Bashkir State Medical University Strategic Academic Leadership Program (PRIORITY-2030).

Availability of data and materials

The datasets used and/or analyzed during the current study are available from the corresponding author on reasonable request.

Authors' contributions

HW, OB and IG made substantial contributions to conception and design and confirm the authenticity of all the raw data RT and AS made substantial contributions to the acquisition of data. XG, AB and TI made substantial contributions to the analysis and interpretation of data. OB and IG were involved in drafting the manuscript or revising it critically for important intellectual content. HW gave final approval for the version published. All authors read and approved the final manuscript and agreed to be accountable for all aspects of the work in ensuring that questions related to the accuracy or integrity of any part of the work are appropriately investigated and resolved.

Ethics approval and consent to participate

The studies involving human participants were reviewed and approved by The approval was provided by the ethics committee of Federal Center of Neurosurgery (Tyumen, Russian Federation). Written informed consent to participate in this study was provided by the participants' legal guardian/next of kin. Written informed consent was obtained from the individual(s), and minor(s)' legal guardian/next of kin, for the publication of any potentially identifiable images or data included in this article.

Patient consent for publication

Not applicable.

Competing interests

The authors declare that they have no competing interests.

References

1. Dolecek TA, Propp JM, Stroup NE and Kruchko C: CBTRUS statistical report: Primary brain and central nervous system tumors diagnosed in the United States in 2005-2009. Neuro Oncol 14 (Suppl 5): v1-49, 2012.
2. Louis DN, Perry A, Wesseling P, Brat DJ, Cree IA, Figarella-Branger D, Hawkins C, Ng HK, Pfister SM, Reifenberger G, *et al*: The 2021 WHO classification of tumors of the central nervous system: A summary. Neuro Oncol 23: 1231-1251, 2021.
3. Olar A, Wani KM, Sulman EP, Mansouri A, Zadeh G and Wilson CD: Mitotic index is an independent predictor of recurrence-free survival in meningioma. Brain Pathol 25: 266-275, 2015.
4. Perry A, Scheithauer BW, Stafford SL, Lohse CM and Wollan PC: 'Malignancy' in meningiomas: A clinicopathologic study of 116 patients, with grading implications. Cancer 85: 2046-2056, 1999.
5. Sughrue ME, Sanai N, Shangari G, Parsa AT, Berger MS and McDermott MW: Outcome and survival following primary and repeat surgery for World Health Organization Grade III meningiomas. J Neurosurg 113: 202-209, 2010.
6. Marciscano AE, Stemmer-Rachamimov AO, Niemierko A, Larvie M, Curry WT, Barker FG II, Martuza RL, McGuone D, Oh KS, Loeffler JS and Shih HA: Benign meningiomas (WHO grade I) with atypical histological features: Correlation of histopathological features with clinical outcomes. J Neurosurg 124: 106-114, 2016.
7. Fox BD, Cheung VJ, Patel AJ, Suki D and Rao G: Epidemiology of metastatic brain tumors. Neurosurg Clin N Am 22: 1-6, v, 2011.
8. Valiente M, Ahluwalia MS, Boire A, Brastianos PK, Goldberg SB, Lee EQ, Le Rhun E, Preusser M, Winkler F and Soffietti R: The evolving landscape of brain metastasis. Trends Cancer 4: 176-196, 2018.
9. Preusser M, Capper D, Ilhan-Mutlu A, Berghoff AS, Birner P, Bartsch R, Marosi C, Zielinski C, Mehta MP, Winkler F, *et al*: Brain metastases: Pathobiology and emerging targeted therapies. Acta Neuropathol 123: 205-222, 2012.
10. Gaspar L, Scott C, Rotman M, Asbell S, Phillips T, Wasserman T, McKenna W and Byhardtl R: Recursive partitioning analysis (RPA) of prognostic factors in three Radiation therapy Oncology Group (RTOG) brain metastases trials. Int J Radiat Oncol Biol Phys 37: 745-751, 1997.

11. Ostrom QT, Gittleman H, Liao P, Vecchione-Koval T, Wolinsky Y, Kruchko C and Barnholtz-Sloan JS: CBTRUS statistical report: Primary brain and other central nervous system tumors diagnosed in the United States in 2010-2014. Neuro Oncol 19 (Suppl_5): v1-v88, 2017.
12. Laigle-Donadey F, Taillibert S, Mokhtari K, Hildebrand J and Delattre JY: Dural metastases. J Neurooncol 75: 57-61, 2005.
13. Gavrilovic IT and Posner JB: Brain metastases: Epidemiology and pathophysiology. J Neurooncol 75: 5-14, 2005.
14. Galldiks N, Angenstein F, Werner JM, Bauer EK, Gutsche R, Fink GR, Langen KJ and Lohmann P: Use of advanced neuroimaging and artificial intelligence in meningiomas. Brain Pathol 32: e13015, 2022.
15. Starr CJ and Cha S: Meningioma mimics: Five key imaging features to differentiate them from meningiomas. Clin Radiol 72: 722-728, 2017.
16. Lyndon D, Lansley JA, Evanson J and Krfishnan AS: Dural masses: Meningiomas and their mimics. Insights Imaging 10: 11, 2019.
17. Rosenberg A and Agulnik M: Epithelioid Hemangioendothelioma: Update on diagnosis and treatment. Curr Treat Options Oncol 19: 19, 2018.
18. Mohan SM, Symss NP, Pande A, Chakravarthy VM and Ramamurthi R: Intracranial epithelioid hemangioendothelioma. Childs Nerv Syst 24: 863-868, 2008.
19. Gamoh S, Tsuno T, Akiyama H, Kotaki S, Nakanishi T, Tsuji K, Yoshida H and Shimizutani K: Intracranial meningeal melanocytoma diagnosed using an interdisciplinary approach: A case report and review of the literature. J Med Case Rep 12: 177, 2018.
20. Barbier EL, Lamalle L and Décorps M: Methodology of brain perfusion imaging. J Magn Reson Imaging 13: 496-520, 2001.
21. Durmo F, Lätt J, Rydelius A, Engelholm S, Kinhult S, Askaner K, Englund E, Bengzon J, Nilsson M, Björkman-Burtscher IM, *et al*: Brain tumor characterization using multibiometric evaluation of MRI. Tomography 4: 14-25, 2018.
22. Saito A, Inoue T, Suzuki S, Ezura M, Uenohara H and Tominaga T: Relationship between pathological characteristics and radiological findings on perfusion MR imaging of meningioma. Neurol Med Chir (Tokyo) 61: 228-235, 2021.
23. Tamrazi B, Shiroishi MS and Liu CS: Advanced imaging of intracranial meningiomas. Neurosurg Clin N Am 27: 137-143, 2016.
24. Kremer S, Grand S, Rémy C, Pasquier B, Benabid AL, Bracard S and Le Bas JF: Contribution of dynamic contrast MR imaging to the differentiation between dural metastasis and meningioma. Neuroradiology 46: 642-648, 2004.
25. Louis DN, Perry A, Reifenberger G, von Deimling A, Figarella-Branger D, Cavenee WK, Ohgaki H, Wiestler OD, Kleihues P and Ellison DW: The 2016 World Health Organization classification of tumors of the central nervous system: A summary. Acta Neuropathol 131: 803-820, 2016.
26. Shibuya M: Pathology and molecular genetics of meningioma: Recent advances. Neurol Med Chir (Tokyo) 55: 14-27, 2015.
27. Boulagnon-Rombi C, Fleury C, Fichel C, Lefour S, Marchal Bressenot A and Gauchotte G: Immunohistochemical approach to the differential diagnosis of meningiomas and their mimics. J Neuropathol Exp Neurol 76: 289, 2017.
28. Wallace E: The dural tail sign. Radiology 233: 56-57, 2004.
29. Zeng L, Liang P, Jiao J, Chen J and Lei T: Will an asymptomatic meningioma grow or not grow? A meta-analysis. J Neurol Surg A Cent Eur Neurosurg 76: 341-347, 2015.
30. O'Leary S, Adams WM, Parrish RW and Mukonoweshuro W: Atypical imaging appearances of intracranial meningiomas. Clin Radiol 62: 10-17, 2007.
31. Kim BW, Kim MS, Kim SW, Chang CH and Kim OL: Peritumoral brain edema in meningiomas: Correlation of radiologic and pathologic features. J Korean Neurosurg Soc 49: 26-30, 2011.
32. Filippi CG, Edgar MA, Uluğ AM, Prowda JC, Heier LA and Zimmerman RD: Appearance of meningiomas on diffusion-weighted images: Correlating diffusion constants with histopathologic findings. AJNR Am J Neuroradiol 22: 65-72, 2001.
33. Nania A, Granata F, Vinci S, Pitrone A, Barresi V, Morabito R, Settineri N, Tomasello F, Alafaci C and Longo M: Necrosis score, surgical time, and transfused blood volume in patients treated with preoperative embolization of intracranial meningiomas. Analysis of a single-centre experience and a review of literature. Clin Neuroradiol 24: 29-36, 2014.
34. Zimny A and Sasiadek M: Contribution of perfusion-weighted magnetic resonance imaging in the differentiation of meningiomas and other extra-axial tumors: Case reports and literature review. J Neurooncol 103: 777-783, 2011.
35. Talybov R, Beylerli O, Mochalov V, Prokopenko A, Ilyasova T, Trofimova T, Sufianov A and Guang Y: Multiparametric MR imaging features of primary CNS lymphomas. Front Surg 9: 887249, 2022.
36. Kremer S, Grand S, Remy C, Esteve F, Lefournier V, Pasquier B, Hoffmann D, Benabid AL and Le Bas JF: Cerebral blood volume mapping by MR imaging in the initial evaluation of brain tumors. J Neuroradiol 29: 105-113, 2002.
37. Nayak L, Abrey LE and Iwamoto FM: Intracranial dural metastases. Cancer 115: 1947-1953, 2009.
38. Seki S, Kamide T, Tamase A, Mori K, Yanagimoto K and Nomura M: Intraparenchymal hemorrhage from dural metastasis of breast cancer mimicking meningioma. Neuroradiol J 29: 179-182, 2016.
39. Furtner J, Oth I, Schöpf V, Nenning KH, Asenbaum U, Wöhrer A, Woitek R, Widhalm G, Kiesel B, Berghoff AS, *et al*: Noninvasive differentiation of meningiomas and dural metastases using intratumoral vascularity obtained by arterial spin labeling. Clin Neuroradiol 30: 599-605, 2020.
40. Fink KR and Fink JR: Imaging of brain metastases. Surg Neurol Int 4: 209-212, 2013.
41. Bendini M, Marton E, Feletti A, Rossi S, Curtolo S, Inches I, Ronzon M, Longatti P and Di Paola F: Primary and metastatic intraaxial brain tumors: Prospective comparison of multivoxel 2D chemical-shift imaging (CSI) proton MR spectroscopy, perfusion MRI, and histopathological findings in a group of 159 patients. Acta Neurochir (Wien) 153:403-412, 2011.
42. Lui YW, Malhotra A, Farinhas JM, Dasari SB, Weidenheim K, Freeman K and LaSala PA: Dynamic perfusion MRI characteristics of Dural metastases and meningiomas: A pilot study characterizing the first-pass wash-in phase beyond relative cerebral blood volume. AJR Am J Roentgenol 196: 886-890, 2011.
43. Shi R, Jiang T, Si L and Li M: Correlations of magnetic resonance, perfusion-weighed imaging parameters and microvessel density in meningioma. J BUON 21: 709-713, 2016.
44. Pillai JJ and Zacá D: Clinical utility of cerebrovascular reactivity mapping in patients with low grade gliomas. World J Clin Oncol 2: 397-403, 2011.
45. Nagesh V, Chenevert TL, Tsien CI, Ross BD, Lawrence TS, Junck L and Cao Y: Quantitative characterization of hemodynamic properties and vasculature dysfunction of high-grade gliomas. NMR Biomed 20: 566-577, 2007.
46. Kremer S, Grand S, Remy C, Esteve F, Lefournier V, Pasquier B, Hoffmann D, Benabid AL and Le Bas JF: Cerebral blood volume mapping by MR imaging in the initial evaluation of brain tumors. J Neuroradiol 29: 105-113, 2002.
47. Toh CH, Wei KC, Chang CN, Peng YW, Ng SH, Wong HF and Lin CP: Assessment of angiographic vascularity of meningiomas with dynamic susceptibility contrast-enhanced perfusion-weighted imaging and diffusion tensor imaging. AJNR Am J Neuroradiol 35: 263-269, 2014.
48. Hakyemez B, Erdogan C, Bolca N, Yildirim N, Gokalp G and Parlak M: Evaluation of different cerebral mass lesions by perfusion-weighted MR imaging. J Magn Reson Imaging 24: 817-824, 2006.
49. Grand S, Tahon F, Attye A, Lefournier V, Le Bas JF and Krainik A: Perfusion imaging in brain disease. Diagn Interv Imaging 94: 1241-1257, 2013.
50. Lin L, Xue Y, Duan Q, Sun B, Lin H, Huang X and Chen X: The role of cerebral blood flow gradient in peritumoral edema for differentiation of glioblastomas from solitary metastatic lesions. Oncotarget 7: 69051-69059, 2016.
51. Hayashida Y, Hirai T, Morishita S, Kitajima M, Murakami R, Korogi Y, Makino K, Nakamura H, Ikushima I, Yamura M, *et al*: Diffusion-weighted imaging of metastatic brain tumors: Comparison with histologic type and tumor cellularity. AJNR Am J Neuroradiol 27: 1419-1425, 2006.
52. Duygulu G, Ovali GY, Calli C, Kitis O, Yünten N, Akalin T and Islekel S: Intracerebral metastasis showing restricted diffusion: Correlation with histopathologic findings. Eur J Radiol 74: 117-120, 2010.
53. Koenig MA: Cerebral edema and elevated intracranial pressure. Continuum (Minneap Minn) 24: 1588-1602, 2018.
54. Esquenazi Y, Lo VP and Lee K: Critical care management of cerebral edema in brain tumors. J Intensive Care Med 32: 15-24, 2017.
55. McKay MJ: Brain metastases: Increasingly precision medicine-a narrative review. Ann Transl Med 9: 1629, 2021.
56. Harrison RA, Nam JY, Weathers SP and DeMonte F: Intracranial Dural, calvarial, and skull base metastases. Handb Clin Neurol 149: 205-225, 2018.